UNIVERSITY OF BRISTOL

Peer reviewed version

Link to published version (if available):
10.1021/acs.nanolett.6b04663

Link to publication record in Explore Bristol Research
PDF-document

University of Bristol - Explore Bristol Research
General rights

Single-molecule transport at a rectifying GaAs contact

Andrea Vezzoli[a], Richard J. Brooke[b], Nicolò Ferri[a], Simon J. Higgins[a], Walther Schwarzacher[b]* and Richard J. Nichols[a]*.

a) Department of Chemistry, University of Liverpool, Crown Street, Liverpool L69 7ZD, UK

b) H. H. Wills Physics Laboratory, University of Bristol, Tyndall Avenue, Bristol BS8 1TL, UK

* Corresponding Authors: nichols@liv.ac.uk and w.schwarzacher@bristol.ac.uk

Table of Contents Graphic
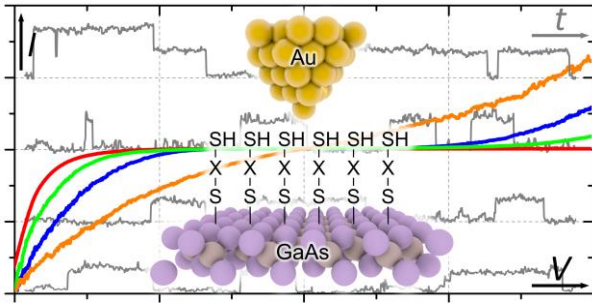
Abstract

In most single- or few-molecule devices, the contact electrodes are simple ohmic resistors. Here we describe a new type of single-molecule device in which metal and semiconductor contact electrodes impart a function, namely current rectification, which is then modified by a molecule bridging the gap. We study junctions with the structure Au STM tip/X/n-GaAs substrate, where 'X' is either a simple alkanedithiol or a conjugated unit bearing thiol/methylthiol contacts, and we detect current jumps corresponding to the attachment and detachment of single molecules. From the magnitudes of the current jumps we can deduce values for the conductance decay constant with molecule length that agree well with values determined from Au/molecule/Au junctions. The ability to impart functionality to a single-molecule device through the properties of the contacts as well as through the properties of the molecule represents a significant extension of the single-molecule electronics 'tool-box'.

Keywords

Main Text

As the density of components on integrated circuits has increased, their dimensions have decreased to just a few nm.[1] At this length-scale, individual organic molecules represent an exceptionally attractive class of component for electronic devices. They are mechanically flexible, insensitive to the manufacturing defects that can affect components produced by conventional top-down lithography, and add functionality such as the ability to respond to environmental stimuli. These can include illumination,[2–5] temperature changes[6–8] and the presence of specific molecules in their surroundings,[9–13] which makes them of special interest for sensor applications. Hybrid organic molecule-inorganic semiconductor devices have the significant advantage that their manufacture could take advantage of the substantial infrastructure investment in the conventional semiconductor industry (where annual expenditure exceeds \$40 billion[14]). However, their development will require a better understanding of the electronic properties of individual molecule-semiconductor interfaces. Although the technological deployment of single molecular junctions would appear to lie a long way off, due to challenges with up-scaling and large-scale fabrication and junction stability, fundamental work is greatly contributing to the understanding of charge transport in molecular junctions and how electrical functionality can be controlled in such junctions. However, combining the properties of semiconducting junctions and single molecules to achieve new functionality has been barely explored and this provides the perspective for the present study.

Organic layers have been fabricated previously on GaAs, as a way to modify the electronic properties of this technologically important surface. For example, organic layers can cause substantial reduction of the surface recombination velocity (SRV)[15] and unpin the surface Fermi level.[16] Furthermore, high

4

quality thiol monolayers on GaAs[17] provide good passivation against oxidation of the surface to Ga_2O_3 / As_2O_3, so that samples are stable for days with minimal increase of XPS Ga $3d_{5/2}$ and As $3d_{5/2}$ oxide signals.[18] Contact angle measurements confirmed the stability of such monolayers for longer periods of time.[19] The electrical properties of relatively large area $(1 - 10 \ \mu m^2)$ Metal / Molecule/ Semiconductor (MMS) devices have been measured previously and are reported extensively in the literature.[20–24] Devices were mainly prepared by depositing a metallic contact on top of a pre-assembled monolayer on a semiconductor, and *I-V* (current-voltage) characteristics are measured to obtain insights into the mechanism of charge transport and device behavior. The deposition of the metallic contact on top of the monolayer is a significant challenge in these devices, as conventional methods such as sputtering or vacuum evaporation can (and often will) damage the molecules or substantially modify the surface in an uncontrollable fashion.[20,25,26] Therefore, alternative methods for the fabrication of MMS devices have been developed, such as soft evaporation[22] and lift-off, float-on (LOFO) of pre-formed metallic pads.[25] However, in all these methods the presence of pinholes in the monolayer can introduce short circuits in the device, thus making the measurements of its properties unreliable.

To overcome these problems, Lee *et al.* used a different approach to measure the properties of a MMS device consisting of a GaAs/dithiol monolayer decorated with Au nanoparticles. By contacting a nanoparticle with a STM probe they were able to collect *I-V* curves and characterize the metal/dithiol/GaAs junction.[23] This method, while advantageous in terms of sample preparation, still has its shortcomings. In particular, the Au nanoparticle needs a stabilizing monolayer on its surface to avoid clustering and sintering, which can introduce additional potential barriers in the device. We reasoned that it would be possible to simply use a Au STM tip to contact the monolayer, thus removing

the need for a nanoparticle and reducing the MMS device complexity. This procedure does indeed generate viable Schottky diodes consisting of an Au STM tip and a GaAs substrate coupled by a small number of molecules connected in parallel. The combination of metal and semiconductor contacts are responsible for the rectifying behavior of our device, as in a conventional metal-insulator-semiconductor diode, while the actual rectification ratio depends on the choice of molecule. Although rectification is a widely studied phenomenon, in both large area and single molecule devices,[26–31] we emphasize here that the rectification in the present case requires both the semiconductor contact and molecule. Furthermore, the current through the device is sensitive to the number of molecules connecting it even though the potential difference across the molecules is only a small fraction of the potential across the complete device, and we can detect the attachment and detachment of *individual* molecules in the device, thus permitting the measurement of properties of single-molecules for the first time in a MMS device.

We focused on three families of molecular wires: (i) simple alkanedithiols (**4DT – 7DT**), (ii) a methylthiol-terminated phenyl ring **1[Ph]1**, where the π-system is decoupled from the contacts, and (iii) a fully-conjugated 4,4'-dithiol-1,1'-biphenyl **BPDT**.
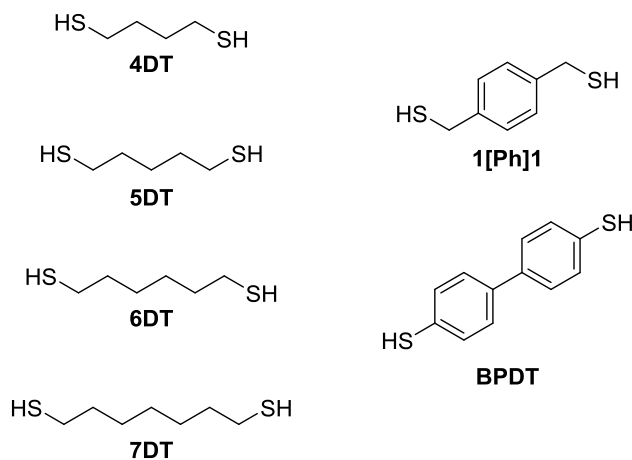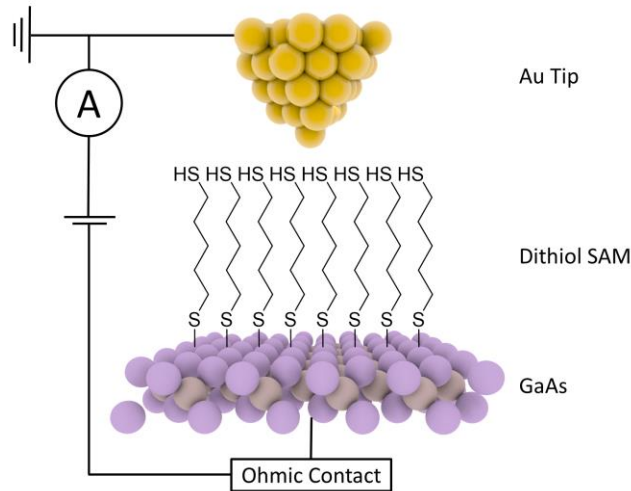
Figure 1: Structures of molecular wires used in this study (top) and schematic of the device used in this study (bottom).

Alkanedithiols on GaAs have already been studied in the literature in conventional (large area) MMS devices[21,22,32] and as uncapped monolayers,[18,19,33] and were found to form densely-packed, defect-free layers and devices. As an archetypal molecular electronics system,[34–36] they were the first subject of our study. In a typical experiment, a gallium-indium eutectic ohmic contact is annealed on the back of a n-type Si-doped <100> GaAs wafer (doping density 3 x 10^{18} cm^{-3}) at 400 °C in vacuum ($\sim$$10^{-2}$ mbar) for 90 minutes. The wafer is then chemically etched (NH$_4$OH 30% in H$_2$O for 5 minutes, followed by DI water rinse) to remove gallium and arsenic native oxides, and then immediately immersed in a degassed ethanol solution containing 1 mM of the desired molecular wire and 5% NH$_4$OH (to avoid oxide layer regrowth and deprotect the thioacetate function in the case of **7DT** and **BPDT**).[37,38] Samples were incubated under Ar atmosphere for 24 hours, removed from solution, thoroughly rinsed with ethanol, dried under a stream of Ar and placed on a Au slide (Arrandee gold-on-glass) with an

additional layer of GaIn eutectic painted to provide optimal contact (schematics of device structure in Figure 1b).

We started our investigation by analyzing the time-dependent tunneling current for 1,6-hexanedithiol (**6DT**) monolayers on GaAs as a function of STM setpoint current I_0. With a low initial I_0 the STM tip is outside the monolayer and the tunneling current profile is flat (green traces, Figure 2a). As I_0 is gradually increased and the electrode separation thereby reduced, the tip comes sufficiently close to the monolayer to interact with it, and Au-S bonds spontaneously form. This results in changes of the tunneling current as the molecular bridges are formed, which we observed as sudden jumps in the current *vs* time profile (red traces, Figure 2a). Similar jumps have been observed for molecular layers on Au and explained by a change in charge transport from tunneling through the bare gap to tunneling through the molecular backbone.[39–41] The measurements of Figure 2 are performed in the dark to avoid the generation of a photocurrent. After finding a setpoint value where the stochastic formation of molecular bridges is evident, the feedback loop was disabled and *I-V* characteristics averaged over 25 different voltage ramps (2 V/s, sweeping from -1 V to 1 V, bias applied to GaAs substrate) were recorded. Under these conditions where *I(t)* jumps are observed the STM tip must be in contact or slightly embedded in the monolayer. Thus the *I-V* curves represent the average charge flow through the STM tip/molecular layer/n-GaAs junction, although at this stage the number of molecules probed in these voltages sweeps is not known (see later). The process was repeated for 1,5-pentanedithiol (**5DT**), 1,4-butanedithiol (**4DT**) and 1,7-heptanedithiol (**7DT**); see Figure 2b and note that these *I-V* curves are normalized, I/I_0, where I_0 is the current at $V_{bias} = -1$ V.
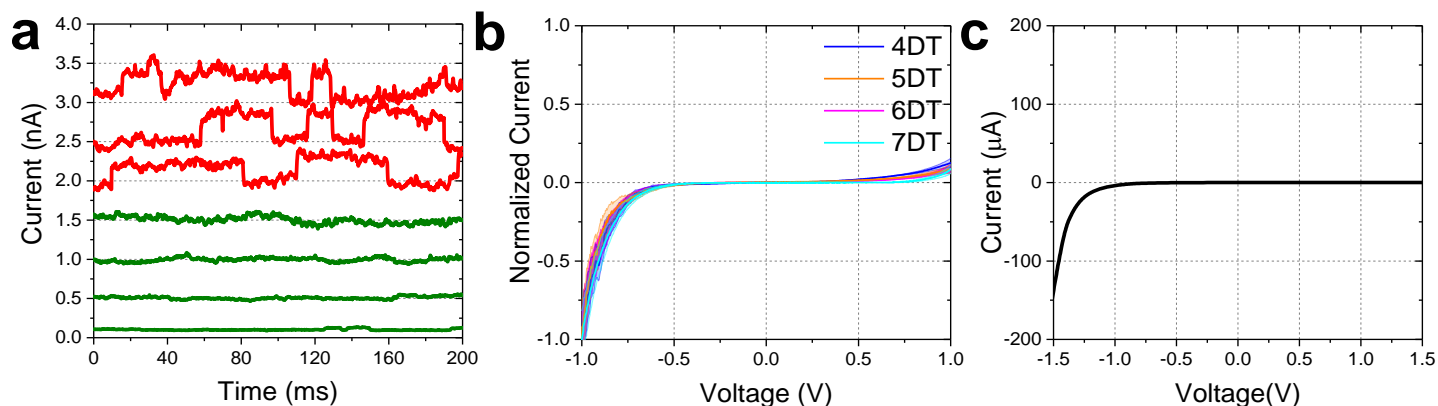
Figure 2: a) Examples of tunneling current as a function of time over a range of setpoint values for **6DT** monolayers on GaAs. b) *I/V* characteristics of MMS devices with alkanedithiols as the molecular bridge. The current is normalized as *I/I$_0$*. See SI for more details. c) *I/V* characteristic of Au tip in direct contact with GaAs substrate (see text).

Our device behaves in the same manner as conventional (large area) MMS devices with alkanedithiols as the organic layer: adding a molecular bridge between the metal and the semiconductor reduces the degree of rectification, as can be observed by comparing the Au-GaAs junction (obtained by crashing the Au tip into a freshly etched GaAs wafer and recording an *I-V* curve, Figure 2c) and MMS devices (Figure 2b). Across the measured series (alkanedithiols **4DT** to **7DT**) there is little change in the rectification ratio RR (*I*(-1 V) / *I*(+1 V) ≈ 12), and this is consistent with a constant barrier height provided by the molecular wires, as already discussed in Au/alkanedithiol/Au junctions.[36,42]

Having established that the electrical behavior measured here using metal STM tip contact is consistent with literature determinations for large-area MMS devices, we moved our focus to molecular systems incorporating conjugated units. We therefore prepared monolayers of **1[Ph]1** and **BPDT**, and measured their properties as MMS junctions (Figure 3). Devices comprising a conjugated molecular bridge behaved in a different manner compared to the alkanedithiols (**7DT**, **6DT**, **5DT** and **4DT**), with

1[Ph]1 showing relatively small rectification (RR ≈ 3.7 at +/- 1 V), consistent with the previously reported near-ohmic behavior of **1[Ph]1** bridging GaAs and a Au nanoparticle.[23] **BPDT** showed further reduced rectification (RR ≈ 1.6 at +/- 1 V), significantly higher currents in forward bias and a more ohmic behavior (in the ± 0.3 V bias window), in good accordance with data obtained on large surface electrodes on fully-conjugated dithiols.[21]
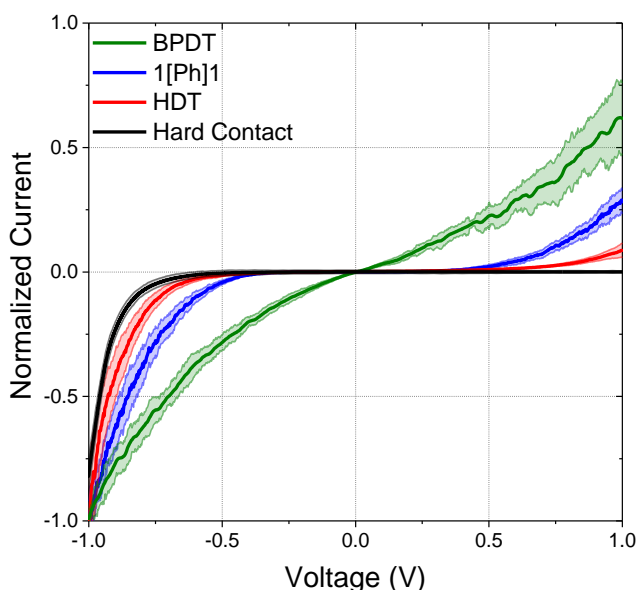

Figure 3: *I/V* characteristics of MMS devices with **1[Ph]1** and **BPDT** as molecular bridge. **6DT** and GaAs/Au "hard" contact as comparison. Current is normalized as *I/I₀*. MMS devices characteristics obtained at 6 nA.

We can model the devices qualitatively as leaky Schottky diodes, with a thin insulating layer between the metal and the semiconductor (the organic monolayer) and surface states at an energy E_{SS} that is fixed relative to the semiconductor band edges, as shown in Figure 4. In forward bias, a relatively large current is attributed to tunneling from E_{SS} to the metal through the molecular bridge by a mechanism similar to that operative in Au-molecule-Au junctions (for the molecules studied here, we expect transport to be dominated by the HOMO in forward bias, *vide infra*), but a substantial limitation to the

current is the barrier height provided by the conduction band bending of the semiconductor (Figure 4). In reverse bias, however, electrons can easily tunnel from the metal to E_{SS} by the same mechanism, but they will be trapped there by the conduction band potential barrier.
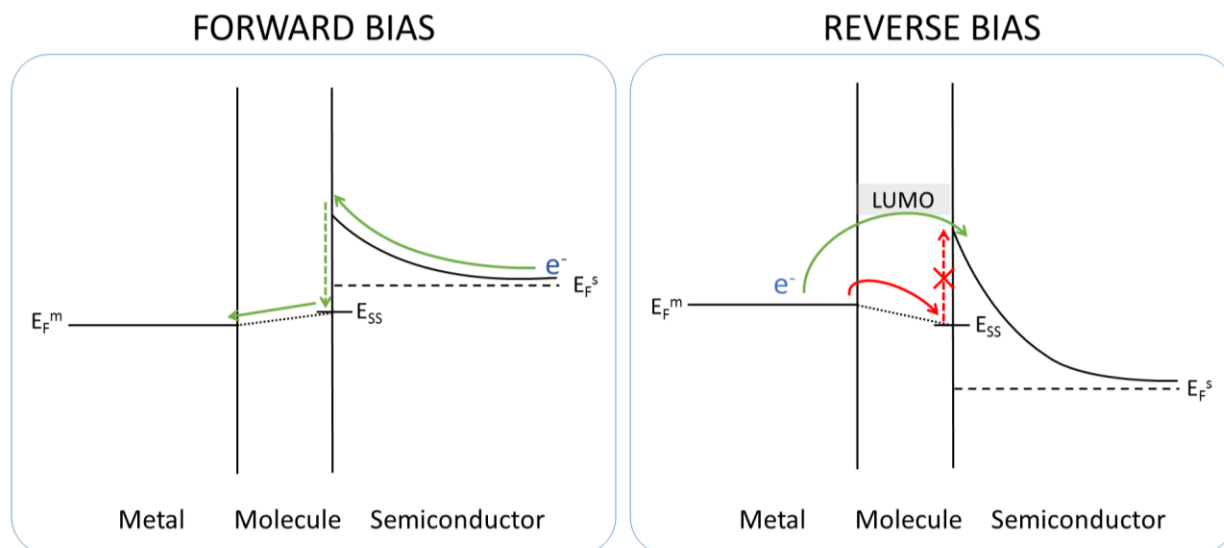

Figure 4: Energy profile of the MMS device under forward (left) and reverse bias (right). A typical literature value of the barrier height for a Au-nGaAs Schottky barrier would be approximately 0.9 eV.[43] With a doping density of 3 x10^{18} cm^{-3}, the semiconductor space charge layer thickness is estimated to be ≈ 20 nm. Dashed arrows refer to the filling or emptying of surface states, while solid lines represent tunneling across the molecular junction.

As the reverse bias voltage is increased, the Fermi level of the metal will approach closer to the molecular LUMO, and the number of electrons tunneling through the molecular orbital directly into the conductance band of the semiconductor (green path on Figure 4) could increase. Therefore, the energy of the LUMO relative to the metal Fermi level is likely key to controlling the current in reverse bias. Molecules with a large HOMO-LUMO gap such as alkanedithiols will have the LUMO far in energy from the metal Fermi level, so that the current in reverse bias will be small, and the device will show a high rectification ratio. As the molecular bridge is made more conjugated in nature, the HOMO-

LUMO gap will reduce in size, and the LUMO be easier to access under reverse bias, thus allowing a larger charge flow and reducing the rectification ratio. A full transport DFT study of the devices presented is outside the scope of this paper, but as a first approach we can use the calculations performed on molecules sandwiched between metal electrodes to estimate the position of the LUMO relative to the Fermi energy of the metal (Figure 5). The position of the LUMO with respect to the metal E_F matches the order of decreasing rectification observed in the MMS devices presented here: the further is the LUMO from the metal E_F, (and thus the bigger is the bandgap) the higher is the rectification ratio.
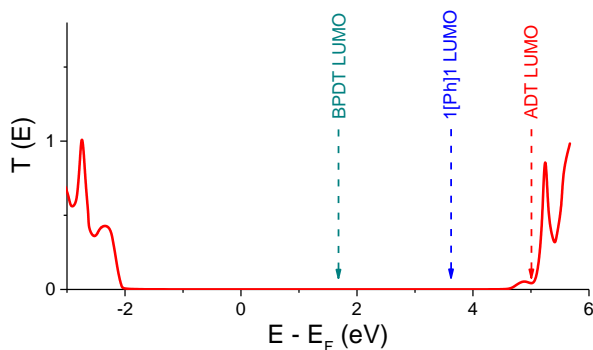

Figure 5: Comparison of the LUMO position for alkanedithiol,[36] 1[Ph]1[44] and BPDT[45] sandwiched between Au electrodes. Data from NEGF-DFT calculations on these systems. The full transmission curve (red) is shown for the alkanedithiol with the foot of the LUMO resonance marked (Copyright 2008 American Chemical Society adapted with permission from reference [36]). 1[Ph]1 and BPDT LUMO positions estimated from references [44] and [45], respectively (see these references for the transmission curves).

The *I-V* curves presented in the preceding text are taken under conditions where the STM tip is in contact with the molecular monolayer on the GaAs substrate, and as such represents current flow through an undefined (albeit small) number of molecules. To characterize single molecule junctions a different approach is required. As discussed previously, when the STM Au tip is close enough to the

dithiol monolayer Au-S bonds can spontaneously form. Under bias voltage, this results in sudden jumps in the current *vs.* time profiles, in a way similar to the established STM technique *I(t)*[46] (also mentioned in the literature as "blinking"[47] or "telegraph noise"[48]) used to characterize charge transport properties of Metal / Molecule / Metal (MMM) junctions. We applied the same technique to the MMS devices we prepared, thus collecting current *vs* time traces containing hundreds of current jumps for each SAM, under forward bias conditions. Taking as an example 1,5-pentanedithiol (**5DT**), using a nominal bias voltage V_{BIAS} of -1 V (we estimate the actual potential difference across the molecular junction is $\sim 0.1 - 0.2$ V due to the voltage drop in the Schottky diode) jumps at 0.56 ± 0.15 and 0.98 ± 0.19 nA are observed, and statistical analysis performed by binning the current jumps in histograms resulted in two peaks (Figure 6). The approximately 2:1 ratio (within error) of the peak heights suggests that the low current feature is when the number of **5DT** molecules bridging the Au-GaAs gap changes by one, while it changes by two molecules bridging the gap for the higher-current one. Measuring current jumps on 1,4-butanedithiol (**4DT**), 1,6-hexanedithiol (**6DT**) and 1,7-heptanedithiol (**7DT**) monolayers on GaAs permitted the calculation of a current decay constant value, as $\beta_L = 0.89 \pm 0.07$ Å^{-1}, or $\beta_N = 1.08 \pm 0.14$ (where N = number of methylene units), in excellent accordance with data published in the literature for Au / alkanedithiol / *Au* junctions.[34,36] This agreement between values for MMS and MMM junctions is consistent with HOMO-based charge transport in forward bias. Due to the low current in reverse bias it was impossible to detect current jumps, and even engaging the STM tip proved difficult. If future measurements are possible in reverse bias and the transport is indeed LUMO-based, it would be interesting to establish the corresponding beta value.
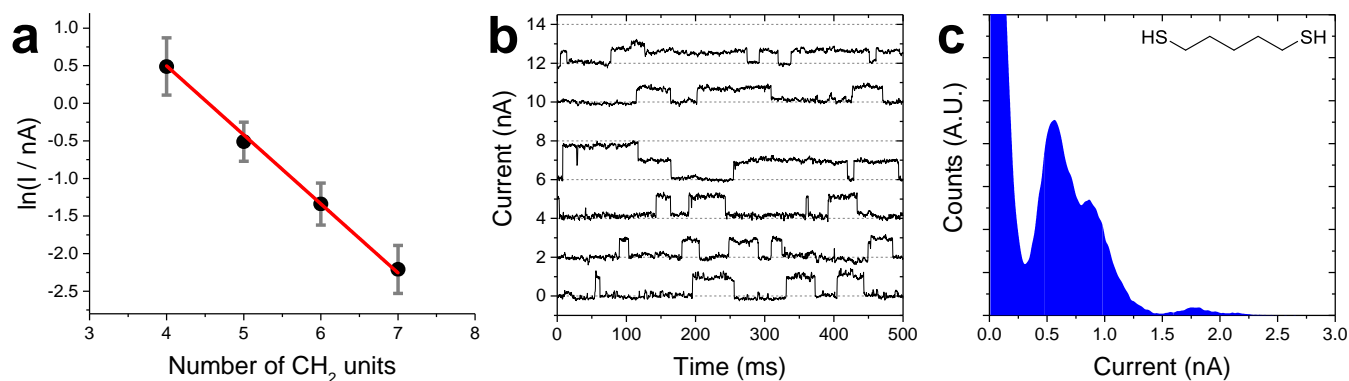
Figure 6: a) Current jumps decay *vs* number of CH_2 units in the molecular wire for the alkanedithiol series. b) Examples of current vs time traces for **5DT** monolayer on GaAs, obtained at 6 nA setpoint, -1 V bias. Traces are shifted on the vertical axis for clarity. c) Statistical histogram compiled from data obtained at 6 nA setpoint, -1 V bias, **5DT** monolayer on GaAs.

To further test the validity of the proposed method and rule out possible effects of the chosen setpoint current I_0 on the magnitude of the current jumps, we performed $I(t)$ measurement at different setpoint current (10 and 20 nA) on **1[Ph]1**, also measured in forward bias. Measurements at higher I_0 resulted in a different distribution of the current jumps (Figure 7), with more of the high-current features that have been attributed to multiple molecules forming and breaking junctions in the semiconductor-metal gap (favoured by the small tip-substrate separation), but the absolute value of the current jumps does not change significantly.
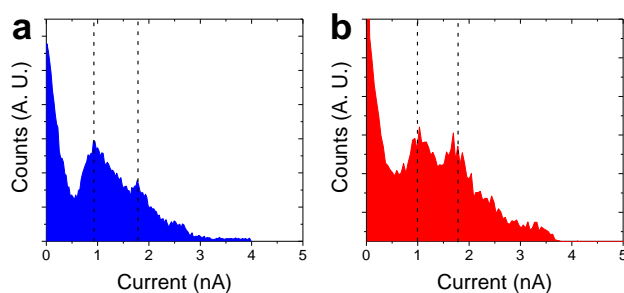
Figure 7: a) Statistical histogram compiled from data obtained at 10 nA setpoint, -1 V bias, **1[Ph]1** monolayer on GaAs. A main peak at 0.92 ± 0.36 nA can be seen, with a satellite peak at 1.79 ± 0.43 nA. b) Statistical histogram compiled from data obtained at 20 nA setpoint, -1 V bias, **1[Ph]1** monolayer on GaAs. Peaks are similar in current values (0.98 ± 0.32 and 1.81 ± 0.54) to the ones obtained at 10 nA, but their ratio is different. A higher setpoint results in closer vicinity of the tip to the substrate, thus increasing the chance of having multiple molecules bridging the gap.

In conclusion, we demonstrate here a hybrid single molecule nanodevice, with gold and GaAs contacts, which functions as a Schottky diode. The combination of metal and semiconductor contacts is responsible for the rectifying behavior of our device, as in a conventional metal-insulator-semiconductor diode, although the rectification ratio RR at +/- 1 V itself depends on the choice of molecule. This combination of contacts, and in particular the band structure of the GaAs contact also suggests a switch from the usual HOMO-mediated conduction mechanism observed metal / alkanedithiol / metal junctions to LUMO-based transport in reverse bias. The electrical behavior of these molecular devices shows strong signatures from the electrical properties of the molecules, in particular the decay constant which is apparently unchanged when the bottom contact is changed from Au to GaAs. This offers attractive prospects for tuning the electrical response of hybrid molecular devices though molecular synthesis.

Methods

Chemicals: 1[Ph]1, **4DT**, **5DT**, **6DT**, solvents and reagents used throughout the syntheses and monolayer preparation were purchased from Sigma-Aldrich and used without further purification. **7DT**[49] and **BPDT**[50] were prepared as bis(thioacetate) following published procedures.

Sample Preparation: In a typical experiment, an ohmic contact (GaIn eutectic, Sigma-Aldrich) is painted on the back of a Si-doped (Si-doped, n-type, <100> ± 0.05°, carrier concentration 3 x 10^{18} cm^{-3}, Wafer Technology Ltd.) <100> GaAs wafer and then annealed at 400 ℃ in vacuum ($\sim 10^{-2}$ mbar) for 90 minutes. The wafer is then chemically etched (NH_4OH 30% in H_2O for 5 minutes, followed by DI water rinse) to remove gallium and arsenide native oxides, and then immediately immersed in a degassed ethanol solution containing 1 mM of the desired molecular wire and 5% NH_4OH (to avoid oxide layer regrowth and deprotect the thioacetate function in **7DT** and **BPDT**).[37,38] Samples were incubated under Ar atmosphere for 24 hours, removed from solution, rinsed with ethanol, dried under a stream of Ar and placed on a Au slide (Arrandee gold-on-glass) with an additional layer of GaIn eutectic painted to provide optimal contact (schematics of device structure in Figure 2).

STM measurements: An STM (Keysight Technologies 5500 SPM) equipped with an electrochemically etched (Ethanol:HCl 37% 1:1, 2.5 V) Au tip (Goodfellow Cambridge Ltd., 99.99+%) was used to fabricate and characterize Au/molecule*/GaAs* junctions. The sample is mounted on the STM stage and the gold tip was advanced towards the substrate and kept at a defined setpoint ($2-20$ nA) at -1 V (substrate negative) nominal bias. The feedback loop was then disabled and current was monitored as a function of time, recording 500 ms traces. When the setpoint current is sufficiently high to allow formation of molecular junctions between the substrate and the tip, current jumps (blinks) are observed, and these jumps have been related to a change in charge transport from tunneling through

air to tunneling through the molecular backbone.[39–41] A typical 500 ms trace contains $3 - 8$ current jumps. Between each trace the feedback loop was turned on to ensure consistent substrate-tip separation throughout the measurements. The STM setup was kept in the dark for the whole duration of the measurements to avoid the generation of a photocurrent. Hundreds of current jumps were collected this way over several hours, and processed using software written in Python which is described in the SI. Automated algorithms are commonly used to process data in single-molecule electronics measurements.[30,51,52] In our software, the background setpoint current was determined and then subtracted from the raw current *vs.* time traces which were afterwards compiled into histograms. Individual traces were broken into segments by locating jumps between the different current levels using features in the differential of the current (*dI/dt*). This was used to produce the current *vs* time density plots (Figures S7 to S10).

Associated Content

Details on data analysis, supporting results (current histograms and traces) and current *vs* time analysis. This material is available free of charge via the internet at http://pubs.acs.org. Raw data is available on the catalog in Liverpool at: http://datacat.liverpool.ac.uk/133/

Author Contributions

A.V. carried out the STM measurements and analyzed the data, with software written by R.J.B.. N.F. and A.V. synthesized the compounds used in this study. R.J.N., S.J.H. and W.S. conceived the experiments and supervised the project. The manuscript was written through contributions of all authors. All authors have given approval to the final version of the manuscript.

Author Information

Corresponding Authors

*E-mail: nichols@liv.ac.uk and w.schwarzacher@bristol.ac.uk

Notes

The authors declare no competing financial interest.

Acknowledgement

References

(1)   Waldrop, M. M. *Nature* **2016**, *530* , 144–147.

(2)   Dulić, D.; van der Molen, S.; Kudernac, T.; Jonkman, H.; de Jong, J.; Bowden, T.; van Esch, J.; Feringa, B.; van Wees, B. *Phys. Rev. Lett.* **2003**, *91*, 207402.

(3)   Martin, S.; Haiss, W.; Higgins, S. J.; Nichols, R. J. *Nano Lett.* **2010**, *10* , 2019–2023.

(4)   Darwish, N.; Aragonès, A. C.; Darwish, T.; Ciampi, S.; Díez-Pérez, I. *Nano Lett.* **2014**, *14*, 7064–7070.

(5)   Tam, E. S.; Parks, J. J.; Shum, W. W.; Zhong, Y.; Santiago-Berríos, M. B.; Zheng, X.; Yang, W.; Chan, G. K.-L.; Abruña, H. D.; Ralph, D. C. *ACS Nano* **2011**, *5*, 5115–5123.

(6)   Luo, L.; Benameur, A.; Brignou, P.; Choi, S. H.; Rigaut, S.; Frisbie, C. D. *J. Phys. Chem. C* **2011**, *115*, 19955–19961.

(7)   Li, X.; Hihath, J.; Chen, F.; Masuda, T.; Zang, L.; Tao, N. *J. Am. Chem. Soc.* **2007**, *129*, 11535–11542.

(8)   Selzer, Y.; Cabassi, M. A.; Mayer, T. S.; Allara, D. L. *J. Am. Chem. Soc.* **2004**, *126*, 4052–4053.

(9)   Vezzoli, A.; Grace, I.; Brooke, C.; Wang, K.; Lambert, C. J.; Xu, B. Q.; Nichols, R. J.; Higgins, S. J. *Nanoscale* **2015**, *7*, 18949–18955.

(10)   Del Re, J.; Moore, M. H.; Ratna, B. R.; Blum, A. S. *Phys. Chem. Chem. Phys.* **2013**, *15*, 8318–8323.

(11)   Milan, D. C.; Al-Owaedi, O. A.; Oerthel, M.-C.; Marqués-González, S.; Brooke, R. J.; Bryce, M. R.; Cea, P.; Ferrer, J.; Higgins, S. J.; Lambert, C. J.; Low, P. J.; Manrique, D. Z.; Martin, S.; Nichols, R. J.; Schwarzacher, W.; García-Suárez, V. M. *J. Phys. Chem. C* **2016**, *120*, 15666–15674.

(12) Nakashima, S.; Takahashi, Y.; Kiguchi, M. *Beilstein J. Nanotechnol.* **2011**, *2*, 755–759.

(13) Zhang, W.; Gan, S.; Vezzoli, A.; Davidson, R. J.; Milan, D. C.; Luzyanin, K. V.; Higgins, S. J.; Nichols, R. J.; Beeby, A.; Low, P. J.; Li, B.; Niu, L. *ACS Nano* **2016**, *10*, 5212–5220.

(14) Grabbi, I.; Blouin, D. *Int. Trade Adm. Dep. Commer. United States Am.* **2015**, No. July.

(15) Rao, V. J.; Manorama, V.; Bhoraskar, S. V. *Appl. Phys. Lett.* **1989**, *54*, 1799–1801.

(16) Carpenter, M. S.; Melloch, M. R.; Dungan, T. E. *Appl. Phys. Lett.* **1988**, *53*, 66–68.

(17) Nakagawa, O. S.; Ashok, S.; Sheen, C. W.; Märtensson, J.; Allara, D. L. *Jpn. J. Appl. Phys.* **1991**, *30*, 3759–3562.

(18) McGuiness, C. L.; Blasini, D.; Masejewski, J. P.; Uppili, S.; Cabarcos, O. M.; Smilgies, D.; Allara, D. L. *ACS Nano* **2007**, *1*, 30–49.

(19) Budz, H. A.; Biesinger, M. C.; LaPierre, R. R. *J. Vac. Sci. Technol. B Microelectron. Nanom. Struct.* **2009**, *27*, 637.

(20) Moons, E.; Bruening, M.; Shanzer, A.; Beier, J.; Cahen, D. *Synth. Met.* **1996**, *76*, 245–248.

(21) Lodha, S.; Janes, D. B. *J. Appl. Phys.* **2006**, *100*, 24503.

(22) Lodha, S.; Janes, D. B. In *4th IEEE Conference on Nanotechnology, 2004.*; IEEE, 2004; pp 278–280.

(23) Lee, T.; Liu, J.; Janes, D. B.; Kolagunta, V. R.; Dicke, J.; Andres, R. P.; Lauterbach, J.; Melloch, M. R.; McInturff, D.; Woodall, J. M.; Reifenberger, R. *Appl. Phys. Lett.* **1999**, *74*, 2869.

(24) Hsu, J. W. P.; Lang, D. V; West, K. W.; Loo, Y.-L.; Halls, M. D.; Raghavachari, K. *J. Phys. Chem. B* **2005**, *109*, 5719–5723.

(25) Vilan, A.; Shanzer, A.; Cahen, D. *Nature* **2000**, *404*, 166–168.

(26) Martin, A. S.; Sambles, J. R.; Ashwell, G. J. *Phys. Rev. Lett.* **1993**, *70*, 218–221.

(27) Metzger, R. M. *Acc. Chem. Res.* **1999**, *32*, 950–957.

(28) Metzger, R. M.; Chen, B.; Höpfner, U.; Lakshmikantham, M. V.; Vuillaume, D.; Kawai, T.; Wu, X.; Tachibana, H.; Hughes, T. V.; Sakurai, H.; Baldwin, J. W.; Hosch, C.; Cava, M. P.; Brehmer, L.; Ashwell, G. J. *J. Am. Chem. Soc.* **1997**, *119*, 10455–10466.

(29) Díez-Pérez, I.; Hihath, J.; Lee, Y.; Yu, L.; Adamska, L.; Kozhushner, M. a; Oleynik, I. I.; Tao, N. *Nat. Chem.* **2009**, *1,* 635–641.

(30) Capozzi, B.; Xia, J.; Adak, O.; Dell, E. J.; Liu, Z.-F.; Taylor, J. C.; Neaton, J. B.; Campos, L. M.; Venkataraman, L. *Nat. Nanotechnol.* **2015**, *10*, 522–527.

(31) Kim, T.; Liu, Z.-F.; Lee, C.; Neaton, J. B.; Venkataraman, L. *Proc. Natl. Acad. Sci.* **2014**, *111*, 10928–10932.

(32) Lodha, S.; Carpenter, P.; Janes, D. B. *J. Appl. Phys.* **2006**, *99*, 24510.

(33) McGuiness, C. L.; Shaporenko, A.; Mars, C. K.; Uppili, S.; Zharnikov, M.; Allara, D. L. *J. Am. Chem. Soc.* **2006**, *128*, 5231–5243.

(34) Li, X.; He, J.; Hihath, J.; Xu, B. Q.; Lindsay, S. M.; Tao, N. J. *J. Am. Chem. Soc.* **2006**, *128*, 2135–2141.

(35) Xu, B. *Science* **2003**, *301*, 1221–1223.

(36) Li, C.; Pobelov, I.; Wandlowski, T.; Bagrets, A.; Arnold, A.; Evers, F. *J. Am. Chem. Soc.* **2008**, *130*, 318–326.

(37) Krapchetov, D. A.; Ma, H.; Jen, A. K. Y.; Fischer, D. A.; Loo, Y. L. *Langmuir* **2008**, *24*, 851–856.

(38) Baum, T.; Ye, S.; Uosaki, K. *Langmuir* **1999**, 24, 8577–8579.

(39) Haiss, W.; Wang, C.; Grace, I.; Batsanov, A. S.; Schiffrin, D. J.; Higgins, S. J.; Bryce, M. R.;

Lambert, C. J.; Nichols, R. J. *Nat. Mater.* **2006**, *5*, 995–1002.

(40)   Huang, S.; He, J.; Chang, S.; Zhang, P.; Liang, F.; Li, S.; Tuchband, M.; Fuhrmann, A.; Ros, R.; Lindsay, S. *Nat. Nanotechnol.* **2010**, *5*, 868–873.

(41)   Chang, S.; He, J.; Kibel, A.; Lee, M.; Sankey, O.; Zhang, P.; Lindsay, S. *Nat. Nanotechnol.* **2009**, *4*, 297–301.

(42)   Pires, E.; Macdonald, J. E.; Elliott, M. *Nanoscale* **2013**, *5*, 9397–9403.

(43)   Rhoderick, E. H.; Williams, R. H. *Metal-semiconductor contacts*; Clarendon Press, 1988.

(44)   Ning, Z.; Chen, J.; Hou, S.; Zhang, J.; Liang, Z.; Zhang, J.; Han, R. *Phys. Rev. B - Condens. Matter Mater. Phys.* **2005**, *72*, 155403.

(45)   Pauly, F.; Viljas, J. K.; Cuevas, J. C.; Schön, G. *Phys. Rev. B* **2008**, *77*, 155312.

(46)   Haiss, W.; Nichols, R. J.; van Zalinge, H.; Higgins, S. J.; Bethell, D.; Schiffrin, D. J. *Phys. Chem. Chem. Phys.* **2004**, *6*, 4330–4337.

(47)   Aragonès, A. C.; Haworth, N. L.; Darwish, N.; Ciampi, S.; Bloomfield, N. J.; Wallace, G. G.; Diez-Perez, I.; Coote, M. L. *Nature* **2016**, *531*, 88–91.

(48)   Chang, S.; He, J.; Lin, L.; Zhang, P.; Liang, F.; Young, M.; Huang, S.; Lindsay, S. *Nanotechnology* **2009**, *20*, 185102.

(49)   Haiss, W.; Martin, S.; Scullion, L. E.; Bouffier, L.; Higgins, S. J.; Nichols, R. J. *Phys. Chem. Chem. Phys.* **2009**, *11*, 10831–10838.

(50)   de Boer, B.; Meng, H.; Perepichka, D. F.; Zheng, J.; Frank, M. M.; Chabal, Y. J.; Bao, Z. *Langmuir* **2003**, *19*, 4272–4284.

(51)   Brooke, R. J.; Jin, C.; Szumski, D. S.; Nichols, R. J.; Mao, B.; Thygesen, K. S.; Schwarzacher, W. *Nano Lett.* **2015**, *15*, 275–280.

(52)   Inkpen, M. S.; Lemmer, M.; Fitzpatrick, N.; Milan, D. C.; Nichols, R. J.; Long, N. J.; Albrecht,

T. *J. Am. Chem. Soc.* **2015**, *137*, 9971–9981.